
Hard-Constrained Neural Networks with Universal Approximation Guarantees

Youngjae Min and Navid Azizan
Massachusetts Institute of Technology

Abstract

Incorporating prior knowledge or specifications of input-output relationships into machine learning models has gained significant attention, as it enhances generalization from limited data and leads to conforming outputs. However, most existing approaches use soft constraints by penalizing violations through regularization, which offers no guarantee of constraint satisfaction—an essential requirement in safety-critical applications. On the other hand, imposing hard constraints on neural networks may hinder their representational power, adversely affecting performance. To address this, we propose **HardNet**, a practical framework for constructing neural networks that inherently satisfy hard constraints without sacrificing model capacity. Unlike approaches that modify outputs only at inference time, **HardNet** enables end-to-end training with hard constraint guarantees, leading to improved performance. To the best of our knowledge, **HardNet** is the first method with an efficient forward pass to enforce more than one input-dependent inequality constraint. It allows unconstrained optimization of the network parameters using standard algorithms by appending a differentiable *closed-form* enforcement layer to the network’s output. Furthermore, we show that **HardNet** retains the universal approximation capabilities of neural networks. We demonstrate the versatility and effectiveness of **HardNet** across various applications: learning with piecewise constraints, learning optimization solvers, optimizing control policies in safety-critical systems, and learning safe decision logic for aircraft systems.¹

1 Introduction

Neural networks are widely adopted for their generalization capabilities and their ability to model highly non-linear functions in high-dimensional spaces. With their increasing proliferation, it has become more important to be able to impose constraints on neural networks in many applications. By incorporating domain knowledge about input-output relationships through constraints, we can enhance generalization, particularly when available data is limited [48, 46, 52]. These constraints introduce inductive biases that guide the model’s learning process toward plausible solutions that adhere to known properties of the problem domain, potentially reducing overfitting. Consequently, neural networks can more effectively capture underlying patterns and make accurate predictions on unseen data, despite scarce training samples.

Moreover, adherence to specific requirements is critical in many practical applications. For instance, in robotics, this could translate to imposing collision avoidance or ensuring configurations remain within a valid motion manifold [18, 67, 53, 31]. In geometric learning, this could mean imposing a manifold constraint [39, 55]. In financial risk management, violating constraints on the solvency of the portfolio can lead to large fines [44]. Enforcing neural network outputs to satisfy these non-negotiable rules (i.e., hard constraints) makes models more reliable, interpretable, and aligned with the underlying problem structure.

¹The code is available at <https://github.com/azizanlab/hardnet>.

However, introducing hard constraints can potentially limit a neural network’s expressive power. To illustrate this point, consider a constraint that requires the model’s output to be less than 1. One could simply restrict the model to always output a constant value less than 1, which ensures the constraint satisfaction but obviously limits the model capacity drastically. This raises the question:

Can we enforce hard constraints on neural networks without losing their expressive power?

The model capacity of neural networks is often explained through the universal approximation theorem, which shows that a neural network can approximate any continuous function given a sufficiently wide/deep architecture. Demonstrating that this theorem still holds under hard constraints is essential to understanding the trade-off between constraint satisfaction and model capacity.

Contributions We tackle the problem of enforcing hard constraints on neural networks by

- **Presenting a practical framework** called **HardNet** (short for hard-constrained neural network) for constructing neural networks that satisfy input-dependent constraints by construction. **HardNet** is, to the best of our knowledge, the first method with an efficient forward pass to enforce more than one input-dependent inequality constraint. It allows for unconstrained optimization of the networks’ parameters with standard algorithms.
- **Proving a universal approximation theorem** for our method, showing that despite enforcing the hard constraints, our construction retains the expressive power of neural networks.
- **Demonstrating the utility** of our method on a variety of scenarios where it is critical to satisfy hard constraints — learning with piecewise constraints, learning optimization solvers, optimizing control policies in safety-critical systems, and learning safe decision logic for aircraft systems.
- **Outlining a survey** of the literature on constructing neural networks that satisfy hard constraints.

2 Related Work

Neural Networks with Soft Constraints Early approaches used data augmentation or domain randomization to structure the dataset to satisfy the necessary constraints before training the neural network. However, this does not ensure constraint satisfaction for arbitrary inputs, especially those far from the training distribution, and outputs often violate constraints marginally even on in-distribution inputs. Other initial directions focused on introducing the constraints as *soft* penalties [43, 17] to the cost function of the neural network along with Lagrange multipliers as hyperparameters. Raissi et al. [52], Li et al. [38] leveraged this idea in their work on physics-informed neural networks (PINNs) to enforce that the output satisfies a given differential equation.

Neural Networks with Hard Constraints Some conventional neural network components can already enforce specific types of hard constraints. For instance, sigmoids can impose lower and upper bounds, softmax layers enforce simplex constraints, and ReLU layers are projections onto the positive orthant. The convolution layer in ConvNets encodes a translational equivariance constraint, which led to significant improvements in empirical performance. Learning new equivariances and inductive biases that accelerate learning for specific tasks is an active research area.

Recent work has explored new architectures to (asymptotically) impose various hard constraints by either finding certain parameterizations of feasible sets or incorporating differentiable projections into neural networks, as summarized in Table 1. Frerix et al. [25] addressed homogeneous linear inequality constraints by embedding a parameterization of the feasible set in a neural network layer. Huang et al. [30] and LinSATNet [66] introduced differentiable projection methods that iteratively refine outputs to satisfy linear constraints. However, these iterative approaches do not guarantee constraint satisfaction within a fixed number of iterations, limiting their reliability in practice. C-DGM [58] enforces linear inequality constraints in generative models for tabular data by incrementally adjusting each output component in a finite number of iterations. However, its application to input-dependent constraints is limited as it cannot efficiently handle batched data. When constraints are input-dependent, the method requires recomputing the reduced constraint sets for each input, making it computationally prohibitive. In the context of optimal power flow, Chen et al. [15] enforces feasibility for learning optimization proxies through closed-form differentiable repair layers. While effective, this approach is restricted to specific affine constraints.

Beyond affine constraints, RAYEN [63] and Konstantinov & Utkin [35] enforce certain convex constraints by parameterizing the feasible set such that the neural network output represents a translation from an interior point of the convex feasible region. However, these methods are limited

Table 1: Comparison of methods enforcing hard constraints on neural networks for the target function $y = f(x) \in \mathbb{R}^{n_{\text{out}}}$. The baselines above the solid midline consider constraints that only depend on the output. For computation, F and B indicate forward and backward passes, respectively. HardNet-Aff is the only method to enforce input-dependent constraints provably and efficiently with universal approximation guarantees.

| Method | Constraint | Satisfaction Guarantee | Computation | Universal Approximator |
|--------------------|--|----------------------------------|------------------|------------------------|
| Frerix et al. [25] | $Ay \leq 0$ | Always | F,B: Closed-Form | Unknown |
| LinSATNet [66] | $A_1y \leq b_1, A_2y \geq b_2, Cy = d$ ($y \in [0, 1]^{n_{\text{out}}}, A_*, b_*, C, d \geq 0$) | Asymptotic | F,B: Iterative | Unknown |
| C-DGM [58] | $Ay \leq \bar{b}$ | Always | F,B: Closed-Form | Unknown |
| RAYEN [63] | $y \in \mathcal{C}$ (\mathcal{C} : linear, quadratic, SOC, LMI) | Always | F,B: Closed-Form | Unknown |
| Soft-Constrained | Any | No | F,B: Closed-Form | Yes |
| POLICE [8] | $y = Ax + b \quad \forall x \in R$ | Always | F,B: Closed-Form | Unknown |
| KKT-hPINN [14] | $Ax + By = b$ (# constraints $\leq n_{\text{out}}$) | Always | F,B: Closed-Form | Unknown |
| ACnet [11] | $h_x(y) = 0$ (# constraints $\leq n_{\text{out}}$) | Always | F,B: Closed-Form | Unknown |
| DC3 [20] | $g_x(y) \leq 0, h_x(y) = 0$ | Asymptotic for linear g_x, h_x | F,B: Iterative | Unknown |
| HardNet-Aff | $A(x)y \leq b(x), C(x)y = d(x)$ (# constraints $\leq n_{\text{out}}$) | Always | F,B: Closed-Form | Yes |

to constraints dependent only on the output, and not the input. Extending these methods to input-dependent constraints is challenging because it requires finding different parameterizations for each input, such as determining a new interior point for every feasible set.

Another line of work considers hard constraints that depend on both input and output. Balestriero & LeCun [8] proposed the POLICE framework for enforcing the output to be an affine function of the input in certain regions of the input space by reformulating the neural networks as continuous piecewise affine mappings. KKT-hPINN [14] enforces more general affine equality constraints by projecting the output to the feasible set where the projection is computed using the KKT conditions of the constraints. ACnet [11] enforces nonlinear equality constraints by transforming the nonlinear constraints to affine constraints for redefined inputs and outputs. However, these methods are limited to enforcing only equality constraints. DC3 [20] is a framework for more general nonlinear constraints that reduces the violations of inequality constraints through gradient-based methods over the manifold where equality constraints are satisfied. However, its constraint satisfaction is not guaranteed in general and is largely affected by the number of gradient steps and the step size, which require fine-tuning.

More closely related to our framework, methods to enforce a single affine inequality constraint have been proposed in the control literature: Kolter & Manek [34] presented a framework for learning a stable dynamical model that satisfies a Lyapunov stability constraint. Based on this method, Min et al. [45] presented the CoLS framework to learn a stabilizing control policy for an unknown control system by enforcing a control Lyapunov stability constraint. Our work generalizes the ideas used in these works to impose more general affine/convex constraints while proving universal approximation guarantees that are absent in prior works; On the theoretical front, Kratsios et al. [36] presented a constrained universal approximation theorem for *probabilistic* transformers whose outputs are constrained to be in a feasible set. However, their contribution is primarily theoretical, and they do not present a method for learning such a probabilistic transformer.

Formal Verification of Neural Networks Verifying whether a provided neural network (after training) always satisfies a set of constraints for a certain set of inputs is a well-studied subject. Albarghouthi et al. [3] provide a comprehensive summary of the constraint-based and abstraction-based approaches to verification. Constraint-based verifiers are often both sound and complete but they have not scaled to practical neural networks, whereas abstraction-based techniques are approximate verifiers which are sound but often incomplete [13, 22, 12, 62, 40, 23, 51, 21]. Other approaches have focused on formally verified exploration and policy learning for reinforcement learning [9, 6, 65]. Contrary to most formal verification methods, which take a pre-trained network and verify that its output always satisfies the desired constraints, our method guarantees constraint satisfaction *by construction* throughout the training.

To address constraint violations in trained models after verification, some methods in safe reinforcement learning introduce shielding mechanisms by overriding unsafe decisions using a backup policy based on reachability analysis [54, 10]. While effective, this setup introduces a hard separation between learning and enforcement, often sacrificing performance and limiting joint optimization. Shielding mechanisms are typically not differentiable and cannot be integrated into training. Similarly, editing methods modify trained networks post hoc to enforce output constraints by solving relaxed optimization problems over the model parameters [56, 60]. Though recent works demonstrate their application during training, these techniques generally target input-independent constraints and are architecture-dependent.

3 Preliminaries

3.1 Notation

For $p \in [1, \infty)$, $\|v\|_p$ denotes the ℓ^p -norm for a vector $v \in \mathbb{R}^m$, and $\|A\|_p$ denotes the operator norm for a matrix $A \in \mathbb{R}^{k \times m}$ induced by the ℓ^p -norm, i.e., $\|A\|_p = \sup_{w \neq 0} \|Aw\|_p / \|w\|_p$. $v_{(i)} \in \mathbb{R}$, $v_{(i)} \in \mathbb{R}^i$, and $v_{(i)} \in \mathbb{R}^{m-i}$ denote the i -th component, the first i and the last $m-i$ components of v , respectively. Similarly, $A_{(i)} \in \mathbb{R}^{k \times i}$ and $A_{(i)} \in \mathbb{R}^{k \times (m-i)}$ denote the first i and the last $m-i$ columns of A , respectively. $[A; B]$ denotes the row-wise concatenation of the matrices A and B .

For a domain $\mathcal{X} \subset \mathbb{R}^{n_{\text{in}}}$ and a codomain $\mathcal{Y} \subset \mathbb{R}^{n_{\text{out}}}$, let $\mathcal{C}(\mathcal{X}, \mathcal{Y})$ be the class of continuous functions from \mathcal{X} to \mathcal{Y} endowed with the sup-norm: $\|f\|_{\infty} := \sup_{x \in \mathcal{X}} \|f(x)\|_{\infty}$. Similarly, $L^p(\mathcal{X}, \mathcal{Y})$ denotes the class of L^p functions from \mathcal{X} to \mathcal{Y} with the L^p -norm: $\|f\|_p := (\int_{\mathcal{X}} \|f(x)\|_p^p dx)^{\frac{1}{p}}$. For function classes $\mathcal{F}_1, \mathcal{F}_2 \subset \mathcal{C}(\mathcal{X}, \mathcal{Y})$ (resp. $\mathcal{F}_1, \mathcal{F}_2 \subset L^p(\mathcal{X}, \mathcal{Y})$), we say \mathcal{F}_1 *universally approximates* (or *is dense in*) a function class \mathcal{F}_2 if for any $f_2 \in \mathcal{F}_2$ and $\epsilon > 0$, there exists $f_1 \in \mathcal{F}_1$ such that $\|f_2 - f_1\|_{\infty} \leq \epsilon$ (resp. $\|f_2 - f_1\|_p \leq \epsilon$). For a neural network, its depth and width are defined as the total number of layers and the maximum number of neurons in any single layer, respectively. Given $x \in \mathcal{X}$, we drop the input dependency on x when it is evident to simplify the presentation.

3.2 Universal Approximation Theorem

The universal approximation property is a foundational concept in understanding the capabilities of neural networks in various applications. Classical results reveal that shallow neural networks with arbitrary width can approximate any continuous function defined on a compact set as formalized in the following theorem [16, 29, 37, 49]:

Theorem 3.1 (Universal Approximation Theorem for Shallow Networks). *Let $\rho : \mathbb{R} \rightarrow \mathbb{R}$ be any continuous function and $\mathcal{K} \in \mathbb{R}$ be a compact set. Then, depth-two neural networks with ρ activation function universally approximate $\mathcal{C}(\mathcal{K}, \mathbb{R})$ if and only if ρ is nonpolynomial.*

To further understand the success of deep learning, the universal approximation property for deep and narrow neural networks has also been studied in the literature [41, 28, 33, 47]. Interesting results show that a critical threshold exists on the width of deep networks that attain the universal approximation property. For instance, deep networks with ReLU activation function with a certain minimum width can approximate any L^p function as described in the following theorem [47, Thm. 1]:

Theorem 3.2 (Universal Approximation Theorem for Deep Networks). *For any $p \in [1, \infty)$, w -width neural networks with ReLU activation function universally approximate $L^p(\mathbb{R}^{n_{\text{in}}}, \mathbb{R}^{n_{\text{out}}})$ if and only if $w \geq \max\{n_{\text{in}} + 1, n_{\text{out}}\}$.*

Despite these powerful approximation guarantees, they fall short when neural networks are required to satisfy hard constraints, such as physical laws or safety requirements. These theorems ensure that a neural network can approximate a target function arbitrarily closely but do not guarantee adherence to necessary constraints. Consequently, even if the target function satisfies specific hard constraints, the neural network approximator might violate them—especially in regions where the target function barely meets the constraints. This shortcoming is particularly problematic for applications that demand strict compliance with non-negotiable domain-specific rules. Therefore, ensuring that neural networks can both approximate target functions accurately and rigorously satisfy hard constraints remains a critical challenge for their deployment in practical applications.

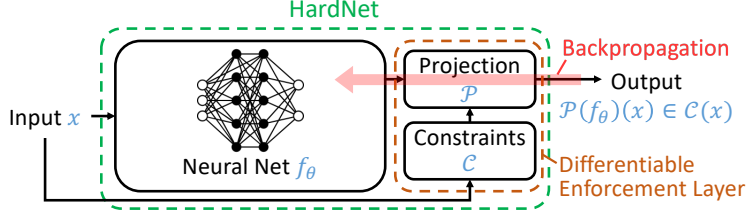


Figure 1: Schematic of HardNet. Its differentiable enforcement layer allows unconstrained end-to-end optimization of the network parameters using standard algorithms while guaranteeing satisfaction with input-dependent constraints by construction. The layer can be applied to any neural networks.

4 HardNet: Hard-Constrained Neural Network

In this section, we present a practical framework HardNet shown in Figure 1 for enforcing input-dependent hard constraints on neural networks while retaining their universal approximation properties. In a nutshell, for a parameterized (neural network) function $f_\theta : \mathcal{X} \subset \mathbb{R}^{n_{\text{in}}} \rightarrow \mathbb{R}^{n_{\text{out}}}$, we ensure the satisfaction of given constraints by appending a differentiable enforcement layer with a projection \mathcal{P} to f_θ . This results in the projected function $\mathcal{P}(f_\theta) : \mathcal{X} \rightarrow \mathbb{R}^{n_{\text{out}}}$ meeting the required constraints while allowing its output to be backpropagated through to train the model via gradient-based algorithms. Importantly, we show that the proposed architecture has universal approximation guarantees, i.e., it universally approximates the class of functions that satisfy the constraints.

A key challenge in this approach is devising a differentiable projection that has efficient forward and backward passes. For instance, consider affine constraints $A(x)f(x) \leq b(x) \forall x \in \mathcal{X}$ for a function $f : \mathcal{X} \rightarrow \mathbb{R}^{n_{\text{out}}}$ with $A(x) \in \mathbb{R}^{n_{\text{ineq}} \times n_{\text{out}}}$ and $b(x) \in \mathbb{R}^{n_{\text{ineq}}}$, one would have

$$\mathcal{P}(f_\theta)(x) = \arg \min_{z \in \mathbb{R}^{n_{\text{out}}}} \|z - f_\theta(x)\|_2 \text{ s.t. } A(x)z \leq b(x). \quad (1)$$

Although the constraints are affine, this projection does not admit a closed-form solution in general, making it expensive to compute—especially as it needs to be computed over every sample x .

In case of a single constraint $a(x)^\top f(x) \leq b(x) \forall x \in \mathcal{X}$ with $a(x) \in \mathbb{R}^{n_{\text{out}}}$ and $b(x) \in \mathbb{R}$, recent work in the control literature—for instance, Kolter & Manek [34] for learning stable dynamics and Donti et al. [19], Min et al. [45] for learning stabilizing controllers—has adopted the following closed-form solution:

$$\mathcal{P}(f_\theta)(x) = \arg \min_{z \in \mathbb{R}^{n_{\text{out}}}} \|z - f_\theta(x)\|_2 \text{ s.t. } a(x)^\top z \leq b(x) \quad (2)$$

$$= f_\theta(x) - \frac{a(x)}{\|a(x)\|^2} \text{ReLU}(a(x)^\top f_\theta(x) - b(x)). \quad (3)$$

This solution is differentiable almost everywhere so that the projected function can be trained using standard optimizers.

Example 4.1. The constraint $(f(x))_{(0)} \geq x(f(x))_{(1)}$ on $f : \mathbb{R} \rightarrow \mathbb{R}^2$ can be encoded as $a(x) = [-1; x]$, $b(x) = 0$ so that a sample $f_\theta(1) = [3; 5]$ is projected to $\mathcal{P}(f_\theta)(1) = [4; 4]$, satisfying the constraint.

Nonetheless, the formulation is limited to enforcing *only a single* inequality constraint. Moreover, its empirical success in learning the desired functions has not been theoretically understood. To that end, we propose HardNet-Aff, the first method to the best of our knowledge, with an efficient forward pass to enforce more than one input-dependent inequality constraint. In addition, we provide a rigorous explanation for its expressivity through universal approximation guarantees. Then, we discuss HardNet-Cvx as a conceptual framework to satisfy general input-dependent convex constraints exploiting differentiable convex optimization solvers.

4.1 HardNet-Aff: Imposing Input-Dependent Affine Constraints

Suppose we have multiple input-dependent affine constraints in an aggregated form:

$$A(x)f(x) \leq b(x), \quad C(x)f(x) = d(x) \quad \forall x \in \mathcal{X}, \quad (4)$$

where $A(x) \in \mathbb{R}^{n_{\text{ineq}} \times n_{\text{out}}}$, $b(x) \in \mathbb{R}^{n_{\text{ineq}}}$, $C(x) \in \mathbb{R}^{n_{\text{eq}} \times n_{\text{out}}}$, $d(x) \in \mathbb{R}^{n_{\text{eq}}}$ for n_{ineq} inequality and n_{eq} equality constraints. For partitions $A(x) = [A_{(:,n_{\text{eq}})} \ A_{(n_{\text{eq}},:)}]$ and $C(x) = [C_{(:,n_{\text{eq}})} \ C_{(n_{\text{eq}},:)}]$, we make the following assumptions about the constraints:

Assumption 4.1. For each $x \in \mathcal{X}$, i) there exists $y \in \mathbb{R}^{n_{\text{out}}}$ that satisfies the constraints in (4), ii) $C_{(:,n_{\text{eq}})}$ is invertible, and iii) $\tilde{A}(x) := A_{(n_{\text{eq}},:)} - A_{(:,n_{\text{eq}})}C_{(:,n_{\text{eq}})}^{-1}C_{(n_{\text{eq}},:)}$ has full row rank.

Given $x \in \mathcal{X}$, when $C(x)$ has full row rank (i.e., no redundant constraints), there exists an invertible submatrix of $C(x)$ with its n_{eq} columns. Without loss of generality, we can assume $C_{(:,n_{\text{eq}})}$ is such submatrix by considering a proper permutation of the components of f . Then, the second assumption holds when the same permutation lets $C_{(:,n_{\text{eq}})}$ invertible for all $x \in \mathcal{X}$. The last assumption requires the total number of the constraints $n_{\text{ineq}} + n_{\text{eq}}$ to be less than or equal to the output dimension n_{out} and $A(x)$ to have full row rank. Also, note that handling the equality constraints separately, instead of viewing them as pairs of inequality constraints $C(x)f(x) \leq d(x)$ and $-C(x)f(x) \leq -d(x)$, is more efficient, because it decreases the total number of constraints from $n_{\text{ineq}} + 2n_{\text{eq}}$ to $n_{\text{ineq}} + n_{\text{eq}}$ and avoids rank-deficient aggregated coefficient $[A(x); C(x); -C(x)]$.

Under the assumptions, we first efficiently reduce the $n_{\text{ineq}} + n_{\text{eq}}$ constraints to n_{ineq} equivalent inequality constraints on partial outputs $f_{(n_{\text{eq}},:)}$ for a partition of the function $f(x) = [f_{(:,n_{\text{eq}})}; f_{(n_{\text{eq}},:)}]$. Consider the hyperplane in the codomain \mathcal{Y} over which the equality constraints are satisfied. Then, for the function output $f(x)$ to be on the hyperplane, the first part $f_{(:,n_{\text{eq}})}$ is determined by $f_{(n_{\text{eq}},:)}$:

$$f_{(:,n_{\text{eq}})}(x) = C_{(:,n_{\text{eq}})}^{-1}(d(x) - C_{(n_{\text{eq}},:)}f_{(n_{\text{eq}},:)}(x)). \quad (5)$$

Substituting this $f_{(:,n_{\text{eq}})}$ into the inequality constraints, the constraints in (4) is equivalent to the following inequality constraints with (5):

$$\underbrace{(A_{(n_{\text{eq}},:)} - A_{(:,n_{\text{eq}})}C_{(:,n_{\text{eq}})}^{-1}C_{(n_{\text{eq}},:)})}_{=: \tilde{A}(x)} f_{(n_{\text{eq}},:)}(x) \leq \underbrace{b(x) - A_{(:,n_{\text{eq}})}C_{(:,n_{\text{eq}})}^{-1}d(x)}_{=: \tilde{b}(x)} \quad \forall x \in \mathcal{X}. \quad (6)$$

With this n_{ineq} equivalent inequality constraints on $f_{(n_{\text{eq}},:)}$, we propose **HardNet-Aff** by developing a novel generalization of the closed-form projection for the single constraint case in (3). Since the first part $f_{(:,n_{\text{eq}})}$ of the function is completely determined by the second part $f_{(n_{\text{eq}},:)}$ as in (5), we let the parameterized function $f_\theta : \mathcal{X} \rightarrow \mathbb{R}^{n_{\text{out}} - n_{\text{eq}}}$ approximate only the second part (or disregard the first n_{eq} outputs if $f_\theta(x) \in \mathbb{R}^{n_{\text{out}}}$ is given). Then, **HardNet-Aff** projects f_θ to satisfy the constraints in (4) as below:

$$\text{HardNet-Aff} : \mathcal{P}(f_\theta)(x) = \left[C_{(:,n_{\text{eq}})}^{-1}(d(x) - C_{(n_{\text{eq}},:)}f_\theta^*(x)); f_\theta^*(x) \right], \quad (7)$$

where $f_\theta^*(x) := f_\theta(x) - \tilde{A}(x)^+ \text{ReLU}(\tilde{A}(x)f_\theta(x) - \tilde{b}(x))$ for all $x \in \mathcal{X}$ with $M^+ := M^\top(MM^\top)^{-1}$ denoting the pseudoinverse of a matrix M . This novel projection satisfies the following properties; see Appendix A.1 for a proof.

Proposition 4.2. *Under Assumption 4.1, for any parameterized (neural network) function $f_\theta : \mathcal{X} \rightarrow \mathbb{R}^{n_{\text{out}} - n_{\text{eq}}}$ and for all $x \in \mathcal{X}$, **HardNet-Aff** $\mathcal{P}(f_\theta)$ in (7) satisfies*

i) $A(x)\mathcal{P}(f_\theta)(x) \leq b(x)$, ii) $C(x)\mathcal{P}(f_\theta)(x) = d(x)$,

iii) For each i -th row $a_i \in \mathbb{R}^{n_{\text{out}}}$ of $A(x)$, $a_i^\top \mathcal{P}(f_\theta)(x) = \begin{cases} a_i^\top \bar{f}_\theta(x) & \text{if } a_i^\top \bar{f}_\theta(x) \leq b_{(i)}(x) \\ b_{(i)}(x) & \text{o.w.} \end{cases}$,

where $\bar{f}_\theta(x) := [[C_{(:,n_{\text{eq}})}^{-1}(d(x) - C_{(n_{\text{eq}},:)}f_\theta(x)); f_\theta(x)] \in \mathbb{R}^{n_{\text{out}}}$.

Remark 4.3 (Parallel Projection). Note that **HardNet-Aff** in (7) for $(n_{\text{ineq}}, n_{\text{eq}}) = (1, 0)$ corresponds to the single-constraint case in (3). However, unlike (3), **HardNet-Aff** in general does not perform the minimum ℓ^2 -norm projection as in (2). Instead, its projection can be understood geometrically via Proposition 4.2 (iii). First, $f_\theta(x)$ is augmented to $\bar{f}_\theta(x)$ to satisfy the equality constraints. If $\bar{f}_\theta(x)$ violates any inequality constraints, it is projected onto the boundary of the feasible set ($a_i^\top \mathcal{P}(f_\theta)(x) = b_{(i)}(x)$). Notably, the projection alters the output in a direction parallel to the boundary of each satisfied constraint's feasible set ($a_i^\top \mathcal{P}(f_\theta)(x) = a_i^\top \bar{f}_\theta(x)$), as shown in Fig. 2.

Remark 4.4 (Gradient Properties). It is worth noting that, for $f_\theta(x)$ initialized outside the feasible set, the enforcement layer can yield zero gradients under certain conditions, even when the projected output differs from the target. However, such cases are infrequent in practice and can be mitigated as

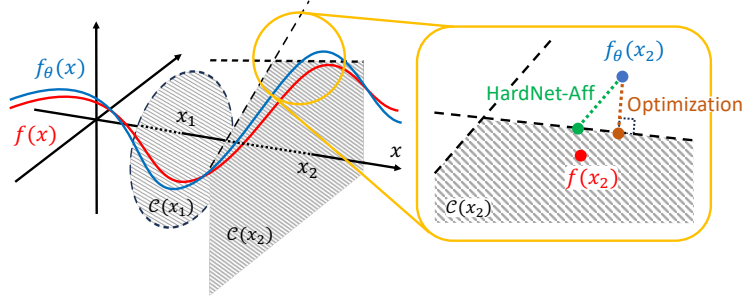


Figure 2: Illustration of input-dependent constraints and projections performed by HardNet. A target function $f : \mathbb{R} \rightarrow \mathbb{R}^2$ satisfies hard constraints $f(x) \in \mathcal{C}(x)$ for each $x \in \mathbb{R}$. The feasible set $\mathcal{C}(x)$ is visualized as the gray area for two sample inputs x_1 and x_2 . While the function f_θ closely approximates f , it violates the constraints. HardNet-Aff projects the violated output onto the feasible set in parallel to the boundaries of the satisfied constraints. In contrast, the minimum ℓ^2 -norm optimization in (1) projects the output orthogonally to the closest boundary.

gradients are averaged over batched data. Thus, HardNet-Aff allows training the projected function to achieve values (strictly) within the feasible set using conventional gradient-based algorithms. Additionally, we can promote the model f_θ to be initialized within the feasible set using the warm-start scheme outlined in Appendix A.5, which involves training the model without the enforcement layer for a few initial epochs while regularizing constraint violations. Further details and discussions are provided in Appendix A.4.

While HardNet-Aff guarantees the satisfaction of the hard constraints (4), it should not lose the neural network’s expressivity for practical deployment. To that end, we rigorously show that HardNet-Aff preserves the neural network’s expressive power by the following universal approximation theorem; see Appendix A.2 for a proof.

Theorem 4.5 (Universal Approximation Theorem with Affine Constraints). *Consider input-dependent constraints (4) that satisfy assumption 4.1. Suppose $\mathcal{X} \subset \mathbb{R}^{n_{\text{in}}}$ is compact, and $A(x), \mathcal{C}(x)$ are continuous over \mathcal{X} . For any $p \in [1, \infty)$, let $\mathcal{F} = \{f \in L^p(\mathcal{X}, \mathbb{R}^{n_{\text{out}}}) \mid f \text{ satisfies (4)}\}$. Then, HardNet-Aff with w -width ReLU neural networks defined in (7) universally approximates \mathcal{F} if $w \geq \max\{n_{\text{in}} + 1, n_{\text{out}} - n_{\text{eq}}\}$.*

The main idea behind this theorem is bounding $\|f - \mathcal{P}(f_\theta)\|$ in terms of $\|f - f_\theta\|$. By selecting f_θ such that $\|f - f_\theta\|$ is arbitrarily small, we can make $\mathcal{P}(f_\theta)$ approach the target function f as closely as desired. The existence of such an f_θ is guaranteed by existing universal approximation theorems. While we utilize Theorem 3.2 in this theorem, other universal approximation theorems on plain neural networks, such as Theorem 3.1, can also be employed.

4.2 HardNet-Cvx: Imposing General Input-Dependent Convex Constraints

Going beyond affine constraints, we discuss HardNet-Cvx as a conceptual framework for enforcing general input-dependent convex constraints $f(x) \in \mathcal{C}(x) \forall x \in \mathcal{X}$ where $\mathcal{C}(x) \subset \mathbb{R}^{n_{\text{out}}}$ is a convex set. Unlike the affine case, the closed-form projection from the single-constraint case in (3) does not extend to general convex constraints. Thus, we present HardNet-Cvx by generalizing the optimization-based projection in (2) as below:

$$\text{HardNet-Cvx} : \mathcal{P}(f_\theta)(x) = \arg \min_{z \in \mathbb{R}^{n_{\text{out}}}} \|z - f_\theta(x)\|_2 \text{ s.t. } z \in \mathcal{C}(x), \quad (8)$$

for all $x \in \mathcal{X}$. While no general closed-form solution for this optimization problem exists, we can employ differentiable convex optimization solvers for an implementation of HardNet-Cvx such as Amos & Kolter [5] for affine constraints (when HardNet-Aff cannot be applied) and Agrawal et al. [1] for more general convex constraints. This idea was briefly mentioned by Donti et al. [20] and used as a baseline (for input-independent constraints) by Tordesillas et al. [63]. However, the computational complexity of such solvers can be a limiting factor in time-sensitive applications. That said, we present HardNet-Cvx as a general framework, independent of specific implementation methods, to complement HardNet-Aff and provide a unified solution for various constraint types.

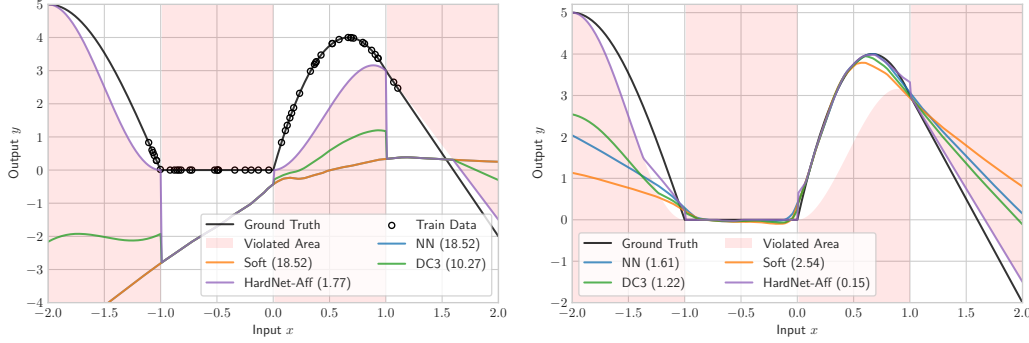


Figure 3: Learned functions at the initial (left) and final (right) epochs with the piecewise constraints. The models are trained on the samples indicated with circles, with their MSE from the true function shown in parentheses. **HardNet-Aff** adheres to the constraints from the start of the training and generalizes better than the baselines on unseen data. On the other hand, the baselines violate the constraints throughout the training.

As in Section 4.1, we demonstrate that **HardNet-Cvx** preserves the expressive power of neural networks by proving the following universal approximation theorem; see Appendix A.3 for a proof.

Theorem 4.6 (Universal Approximation Theorem with Convex Constraints). *Consider input-dependent constrained sets $\mathcal{C}(x) \subset \mathbb{R}^{n_{\text{out}}}$ that are convex for all $x \in \mathcal{X} \subset \mathbb{R}^{n_{\text{in}}}$. For any $p \in [1, \infty)$, let $\mathcal{F} = \{f \in L^p(\mathcal{X}, \mathbb{R}^{n_{\text{out}}}) \mid f(x) \in \mathcal{C}(x) \forall x \in \mathcal{X}\}$. Then, **HardNet-Cvx** with w -width ReLU neural networks defined in (8) universally approximates \mathcal{F} if $w \geq \max\{n_{\text{in}} + 1, n_{\text{out}}\}$.*

5 Experiments

In this section, we demonstrate the versatility and effectiveness of **HardNet-Aff** over three constrained scenarios: learning with piecewise constraints, learning optimization solvers, and optimizing control policies in safety-critical systems. An additional scenario of learning safe decision logic for aircraft systems is introduced in Appendix A.8.

As evaluation metrics, we measure the violation of constraints in addition to the application-specific performance metrics. For a test sample $x \in \mathcal{X}$ and n_{ineq} inequality constraints $g_x(f(x)) \leq 0 \in \mathbb{R}^{n_{\text{ineq}}}$, their violation is measured with the maximum ($\leq \max$) and mean ($\leq \text{mean}$) of $\text{ReLU}(g_x(f(x)))$ and the number of violated constraints ($\leq \#$). Similar quantities of $|h_x(f(x))|$ are measured for n_{eq} equality constraints $h_x(f(x)) = 0 \in \mathbb{R}^{n_{\text{eq}}}$. Then, they are averaged over all test samples. The inference time (T_{test}) for the test set and the training time (T_{train}) are also compared.

We compare **HardNet** with the following baselines: (i) **NN**: Plain neural networks, (ii) **Soft**: Soft-constrained neural networks, where constraint violations are penalized by adding regularization terms $\lambda_{\leq} \|\text{ReLU}(g_x(f(x_s)))\|_2^2 + \lambda_{=} \|h_x(f(x_s))\|_2^2$ to the loss function for each sample $x_s \in \mathcal{X}$, (iii) **DC3** [20]: Similarly to **HardNet-Aff**, DC3 approximates part of the target function with a neural network. It first augments the output to satisfy equality constraints, then corrects it using gradient descent to minimize inequality violations. DC3 backpropagates through this iterative correction procedure to train the model. All methods use 3-layer fully connected neural networks with 200 neurons per hidden layer and ReLU activation.

5.1 Learning with Piecewise Constraints

In this experiment, we demonstrate the efficacy of **HardNet-Aff** and the expressive power of input-dependent constraints on a problem involving learning a function $f : [-2, 2] \rightarrow \mathbb{R}$ with piecewise constraints shown in Fig. 3. The function outputs are required to avoid specific regions defined over separate subsets of the domain $[-2, 2]$. An arbitrary number of such piecewise constraints can be captured by a single input-dependent affine constraint. The models are trained on 50 labeled data points randomly sampled from $[-1.2, 1.2]$; see Appendix A.6 for details.

Table 2: Results for the function fitting experiment. **HardNet-Aff** generalizes better than the baselines with the smallest MSE from the true function without any constraint violation. The max, mean, and the number of constraint violations are computed out of 401 test samples. Violations are highlighted in red. Standard deviations over 5 runs are shown in parentheses.

| | MSE | $\not\leq$ max/mean/# | T_{test} (ms) | T_{train} (s) |
|--------------------|-------------|---|------------------------|------------------------|
| NN | 1.85 (0.19) | 3.16/0.60/212.2 (0.29/0.04/7.19) | 1.7 (0.01) | 1.97 (0.02) |
| Soft | 2.36 (0.22) | 3.70/0.69/205.2 (0.25/0.03/1.94) | 1.64 (0.08) | 2.13 (0.12) |
| DC3 | 1.15 (0.10) | 2.31/0.43/207.0 (0.23/0.02/3.58) | 38.69 (0.33) | 14.14 (0.47) |
| HardNet-Aff | 0.16 (0.01) | 0/0/0 (0/0/0) | 6.38 (0.67) | 4.48 (0.16) |

Table 3: Results for learning solvers of nonconvex optimization problems with 100 variables, 50 equality constraints, and 50 inequality constraints. **HardNet-Aff** attain feasible solutions with the smallest suboptimality gap among the feasible methods. The max, mean, and the number of violations are computed out of the 50 constraints. Violations are highlighted in red. Standard deviations over 5 runs are shown in parentheses.

| | Obj. val | $\not\leq$ max/mean/# | \neq max/mean/# | T_{test} (ms) | T_{train} (s) |
|--------------------|---------------|--|---|------------------------|------------------------|
| Optimizer | -14.28 (0.00) | 0/0/0 (0/0/0) | 0/0/0 (0/0/0) | 988.8 (5.74) | - |
| NN | -27.42 (0.00) | 11.83/1.07/11.99 (0.03/0.00/0.01) | 14.91/6.32/50 (0.01/0.00/0) | 5.68 (1.52) | 35.59 (1.58) |
| Soft | -12.08 (0.04) | 0.00/0.00/0.00 (0.00/0.00/0.00) | 0.46/0.17/49.98 (0.00/0.00/0.00) | 6.34 (1.59) | 35.51 (1.40) |
| DC3 | -12.96 (0.05) | 0.00/0.00/0.00 (0.00/0.00/0.00) | 0.00/0.00/0.00 (0.00/0.00/0.00) | 87.67 (2.40) | 619.7 (9.16) |
| HardNet-Aff | -13.79 (0.13) | 0/0/0 (0/0/0) | 0/0/0 (0/0/0) | 25.58 (4.76) | 189.3 (1.95) |

As shown in Fig. 3 and Table 2, **HardNet-Aff** consistently satisfies the hard constraints throughout training and achieves better generalization than the baselines, which violate these constraints. Especially at the boundaries $x = -1$ and $x = 1$ in the initial epoch results, the jumps in DC3’s output value, caused by DC3’s correction process, insufficiently reduce the constraint violations. The performance of its iterative correction process heavily depends on the number of gradient descent steps and the step size. DC3 requires careful hyperparameter tuning unlike **HardNet-Aff**.

5.2 Learning Optimization Solver

We consider the problem of learning optimization solvers as in Donti et al. [20] with the following nonconvex optimization problem:

$$f(x) = \arg \min_y \frac{1}{2} y^\top Q y + p^\top \sin y \quad \text{s.t. } Ay \leq b, Cy = x, \quad (9)$$

where $Q \in \mathbb{R}^{n_{\text{out}} \times n_{\text{out}}} \succeq 0$, $p \in \mathbb{R}^{n_{\text{out}}}$, $A \in \mathbb{R}^{n_{\text{ineq}} \times n_{\text{out}}}$, $b \in \mathbb{R}^{n_{\text{ineq}}}$, $C \in \mathbb{R}^{n_{\text{eq}} \times n_{\text{out}}}$ are constants and \sin is the element-wise sine function. The target function f outputs the solution of each optimization problem instance determined by the input $x \in [-1, 1]^{n_{\text{eq}}}$. The main benefit of learning this nonconvex optimization solver with neural networks is their faster inference time than optimizers based on iterative methods. To ensure that the learned neural networks provide feasible solutions, the constraints of the optimization problems are set as hard constraints.

In this experiment, we guarantee that the given constraints are feasible for all $x \in [-1, 1]^{n_{\text{eq}}}$ by computing a proper b for randomly generated A, C as described in Donti et al. [20]. Then the models are trained on 10000 unlabeled data points uniformly sampled from $[-1, 1]^{n_{\text{eq}}}$. To perform this unsupervised learning task, the loss function for each sample x_s is set as $\frac{1}{2} f_\theta(x_s)^\top Q f_\theta(x_s) + p^\top \sin f_\theta(x_s)$. To reproduce similar results as in Donti et al. [20], the models are equipped with additional batch normalization and dropout layers in this experiment. As shown in Table 3, **HardNet-Aff** consistently finds feasible solutions with a small suboptimality gap from the optimizer (IPOPT) with a much shorter inference time.

5.3 Optimizing Control Policy in Safety-Critical System

In this experiment, we apply **HardNet-Aff** to enforce safety constraints in control systems. Consider a control-affine system with its known dynamics f and g : $\dot{x}(t) = f(x(t)) + g(x(t))u(t)$,

Table 4: Results for optimizing safe control policies. **HardNet-Aff** generates trajectories without constraint violation and has the smallest costs among the methods with zero violation. The max and mean constraint violations are computed for the violations accumulated throughout the trajectories. Violations are highlighted in red. Standard deviations over 5 runs are shown in parentheses.

| | Cost | $\not\leq$ max/mean | T_{test} (ms) | T_{train} (min) |
|-------------|---------------|---------------------------|------------------------|--------------------------|
| NN | 421.92 (0.15) | 157.62/118.92 (0.90/0.55) | 0.49 (0.11) | 180.22 (1.25) |
| Soft | 480.10 (0.54) | 6.92/3.95 (0.05/0.10) | 0.89 (0.76) | 180.10 (0.58) |
| DC3 | 480.12 (0.59) | 6.90/3.93 (0.08/0.13) | 24.17 (3.18) | 758.50 (61.96) |
| HardNet-Aff | 518.85 (8.71) | 0/0 (0/0) | 3.16 (0.32) | 239.69 (1.46) |

where $x(t) \in \mathbb{R}^{n_{\text{in}}}$ and $u(t) \in \mathbb{R}^{n_{\text{out}}}$ are the system state and the control input at time t , respectively. For safety reasons (e.g., avoiding obstacles), the system requires $x(t) \in \mathcal{X}_{\text{safe}} \subset \mathbb{R}^{n_{\text{in}}}$ for all t . We translate this safety condition into a state-dependent affine constraint on the control input using a control barrier function (CBF) $h : \mathbb{R}^{n_{\text{in}}} \rightarrow \mathbb{R}$ [4]. Suppose its super-level set $\{x \in \mathbb{R}^{n_{\text{in}}} | h(x) \geq 0\} \subset \mathcal{X}_{\text{safe}}$ and $h(x(0)) \geq 0$. Then, we can ensure $h(x(t)) \geq 0 \forall t \geq 0$ by guaranteeing

$$\dot{h}(x) = \nabla h(x)^\top (f(x) + g(x)\pi(x)) \geq -\alpha h(x) \quad (10)$$

at each $x(t)$ for a state-feedback control policy $\pi : \mathbb{R}^{n_{\text{in}}} \rightarrow \mathbb{R}^{n_{\text{out}}}$ with some $\alpha > 0$. Enforcing (10) for multiple CBFs ensures the trajectory remains within the intersection of the corresponding safe sets.

We consider controlling a unicycle system to minimize the cost over trajectories while avoiding collisions with two elliptical obstacles, each presented with a CBF (see Appendix A.7 for details). Then, we can formulate the problem as an optimization problem with its objective function being the expected cost over the trajectory $x(t)$ generated by a parameterized state feedback policy $\pi_\theta : \mathbb{R}^{n_{\text{in}}} \rightarrow \mathbb{R}^{n_{\text{out}}}$ from random initial point $x(0) \sim \mathcal{D}$:

$$\arg \min_{\theta} \mathbb{E}_{x(0) \sim \mathcal{D}} \int_{t=0}^T [x^\top Q x + \pi_\theta(x)^\top R \pi_\theta(x)] dt \quad \text{s.t. (10) holds for all CBFs } \forall t \in [0, T] \forall i \quad (11)$$

where Q is the state cost matrix and R is the control cost matrix.

Given a nominal controller $\pi_{\text{nom}} : \mathbb{R}^{n_{\text{in}}} \rightarrow \mathbb{R}^{n_{\text{out}}}$ designed without obstacle considerations, a conventional approach to find a safe controller is to solve the following quadratic program at each $x(t)$:

$$\text{CBF-QP} : \pi_{\text{CBF-QP}}(x) = \arg \min_u \|u - \pi_{\text{nom}}(x)\|_2 \quad \text{s.t. (10) holds for all CBFs.} \quad (12)$$

The downside of this method is that the controller cannot optimize a cost/reward over trajectories, as it only stays close to the nominal controller. Instead, we can do so by training neural network policies $\pi_\theta(x) := \pi_{\text{nom}}(x) + f_\theta(x)$ with neural networks f_θ . For computation, we approximate (11) by minimizing the costs of rolled-out trajectories from randomly sampled initial states. As shown in Fig. 4 and Table 4, **HardNet-Aff** consistently guarantees safe trajectories with low costs.

6 Conclusion

In this paper, we presented **HardNet**, a practical framework for constructing neural networks that inherently satisfy input-dependent affine/convex constraints. We proved that imposing these hard constraints does not limit the expressive power of these neural networks by providing universal

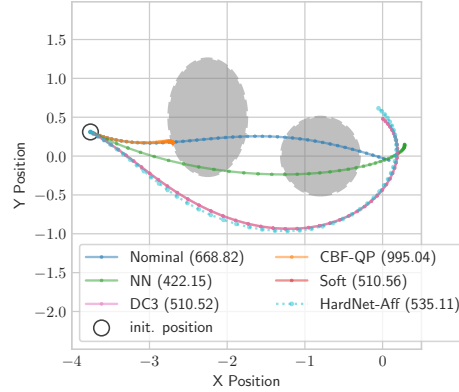


Figure 4: Simulated trajectories from a random initial state, with costs shown in parentheses. **HardNet-Aff** avoids the obstacles while obtaining a low cost value. Even though the soft-constrained method and DC3 appear to avoid obstacles and achieve smaller costs than the other collision-free trajectories, they violate the safety constraints (which are more conservative than hitting the obstacles).

approximation guarantees. We demonstrated the utility and versatility of our method across several applications, such as learning with piecewise constraints, learning optimization solvers, and optimizing control policies in safety-critical systems. Using HardNet in other application domains that benefit from incorporating domain-specific knowledge is a promising direction for future work. One such example is in [59]. Also, we aim to explore developing methods for performing fast projections for problems with more general constraints. Lastly, extending our approach to support other forms of inductive biases, such as equivariances and invariances, would potentially be of great interest.

Acknowledgments

The authors thank Anoopkumar Sonar for discussions and helpful input on an early version of this manuscript. The authors acknowledge the MIT SuperCloud and Lincoln Laboratory Supercomputing Center for providing computing resources that have contributed to the results reported within this paper. This work was supported in part by MathWorks, the MIT-IBM Watson AI Lab, the MIT-Amazon Science Hub, and the MIT-Google Program for Computing Innovation.

References

- [1] Agrawal, A., Amos, B., Barratt, S., Boyd, S., Diamond, S., and Kolter, J. Z. Differentiable convex optimization layers. *Advances in neural information processing systems*, 32, 2019.
- [2] Ahmed, K., Teso, S., Chang, K.-W., Van den Broeck, G., and Vergari, A. Semantic probabilistic layers for neuro-symbolic learning. *Advances in Neural Information Processing Systems*, 35: 29944–29959, 2022.
- [3] Albarghouthi, A. et al. Introduction to neural network verification. *Foundations and Trends® in Programming Languages*, 7(1–2):1–157, 2021.
- [4] Ames, A. D., Coogan, S., Egerstedt, M., Notomista, G., Sreenath, K., and Tabuada, P. Control barrier functions: Theory and applications. In *2019 18th European control conference (ECC)*, pp. 3420–3431. IEEE, 2019.
- [5] Amos, B. and Kolter, J. Z. Optnet: Differentiable optimization as a layer in neural networks. In *International Conference on Machine Learning*, pp. 136–145. PMLR, 2017.
- [6] Anderson, G., Verma, A., Dillig, I., and Chaudhuri, S. Neurosymbolic reinforcement learning with formally verified exploration. *Advances in neural information processing systems*, 33: 6172–6183, 2020.
- [7] Badreddine, S., Garcez, A. d., Serafini, L., and Spranger, M. Logic tensor networks. *Artificial Intelligence*, 303:103649, 2022.
- [8] Balestrierio, R. and LeCun, Y. Police: Provably optimal linear constraint enforcement for deep neural networks. In *ICASSP 2023-2023 IEEE International Conference on Acoustics, Speech and Signal Processing (ICASSP)*, pp. 1–5. IEEE, 2023.
- [9] Bastani, O., Pu, Y., and Solar-Lezama, A. Verifiable reinforcement learning via policy extraction. *Advances in neural information processing systems*, 31, 2018.
- [10] Bastani, O., Li, S., and Xu, A. Safe reinforcement learning via statistical model predictive shielding. In *Robotics: Science and Systems*, pp. 1–13, 2021.
- [11] Beucler, T., Pritchard, M., Rasp, S., Ott, J., Baldi, P., and Gentine, P. Enforcing analytic constraints in neural networks emulating physical systems. *Physical review letters*, 126(9): 098302, 2021.
- [12] Brown, R. A., Schmerling, E., Azizan, N., and Pavone, M. A unified view of sdp-based neural network verification through completely positive programming. In *International conference on artificial intelligence and statistics*, pp. 9334–9355. PMLR, 2022.
- [13] Bunel, R., Turkaslan, I., Torr, P. H., Kohli, P., and Kumar, M. P. A unified view of piecewise linear neural network verification. In *Proceedings of the 32nd International Conference on Neural Information Processing Systems, NIPS’18*, pp. 4795–4804. Curran Associates Inc., 2018.

- [14] Chen, H., Flores, G. E. C., and Li, C. Physics-informed neural networks with hard linear equality constraints. *Computers & Chemical Engineering*, 189:108764, 2024.
- [15] Chen, W., Tanneau, M., and Van Hentenryck, P. End-to-end feasible optimization proxies for large-scale economic dispatch. *IEEE Transactions on Power Systems*, 39(2):4723–4734, 2023.
- [16] Cybenko, G. Approximation by superpositions of a sigmoidal function. *Mathematics of control, signals and systems*, 2(4):303–314, 1989.
- [17] Dener, A., Miller, M. A., Churchill, R. M., Munson, T., and Chang, C.-S. Training neural networks under physical constraints using a stochastic augmented lagrangian approach. *arXiv preprint arXiv:2009.07330*, 2020.
- [18] Ding, M. and Fan, G. Multilayer joint gait-pose manifolds for human gait motion modeling. *IEEE Transactions on Cybernetics*, 45(11):2413–2424, 2014.
- [19] Donti, P. L., Roderick, M., Fazlyab, M., and Kolter, J. Z. Enforcing robust control guarantees within neural network policies. In *International Conference on Learning Representations*, 2021.
- [20] Donti, P. L., Rolnick, D., and Kolter, J. Z. DC3: A learning method for optimization with hard constraints. In *International Conference on Learning Representations*, 2021.
- [21] Ehlers, R. Formal verification of piece-wise linear feed-forward neural networks. In *Automated Technology for Verification and Analysis: 15th International Symposium, ATVA 2017, Pune, India, October 3–6, 2017, Proceedings 15*, pp. 269–286. Springer, 2017.
- [22] Elboher, Y. Y., Gottschlich, J., and Katz, G. An abstraction-based framework for neural network verification. In *Computer Aided Verification: 32nd International Conference, CAV 2020, Los Angeles, CA, USA, July 21–24, 2020, Proceedings, Part I*, pp. 43–65. Springer-Verlag, 2020. ISBN 978-3-030-53287-1. doi: 10.1007/978-3-030-53288-8_3.
- [23] Fazlyab, M., Morari, M., and Pappas, G. J. Safety verification and robustness analysis of neural networks via quadratic constraints and semidefinite programming. *IEEE Transactions on Automatic Control*, 67(1):1–15, 2020.
- [24] Fischer, M., Balunovic, M., Drachler-Cohen, D., Gehr, T., Zhang, C., and Vechev, M. D12: training and querying neural networks with logic. In *International Conference on Machine Learning*, pp. 1931–1941. PMLR, 2019.
- [25] Frerix, T., Nießner, M., and Cremers, D. Homogeneous linear inequality constraints for neural network activations. In *Proceedings of the IEEE/CVF Conference on Computer Vision and Pattern Recognition Workshops*, pp. 748–749, 2020.
- [26] Giunchiglia, E. and Lukasiewicz, T. Coherent hierarchical multi-label classification networks. *Advances in neural information processing systems*, 33:9662–9673, 2020.
- [27] Giunchiglia, E., Tatomir, A., Stoian, M. C., and Lukasiewicz, T. Ccn+: A neuro-symbolic framework for deep learning with requirements. *International Journal of Approximate Reasoning*, pp. 109124, 2024.
- [28] Hanin, B. and Sellke, M. Approximating continuous functions by relu nets of minimal width. *arXiv preprint arXiv:1710.11278*, 2017.
- [29] Hornik, K., Stinchcombe, M., and White, H. Multilayer feedforward networks are universal approximators. *Neural networks*, 2(5):359–366, 1989.
- [30] Huang, D., Zhang, H., Song, X., and Shibasaki, R. Differentiable projection for constrained deep learning. *arXiv preprint arXiv:2111.10785*, 2021.
- [31] Huang, H., Wang, D., Walters, R., and Platt, R. Equivariant transporter network. *arXiv preprint arXiv:2202.09400*, 2022.

- [32] Katz, G., Barrett, C., Dill, D. L., Julian, K., and Kochenderfer, M. J. Reluplex: An efficient smt solver for verifying deep neural networks. In *Computer Aided Verification: 29th International Conference, CAV 2017, Heidelberg, Germany, July 24-28, 2017, Proceedings, Part I* 30, pp. 97–117. Springer, 2017.
- [33] Kidger, P. and Lyons, T. Universal approximation with deep narrow networks. In *Conference on learning theory*, pp. 2306–2327. PMLR, 2020.
- [34] Kolter, J. Z. and Manek, G. Learning stable deep dynamics models. *Advances in neural information processing systems*, 32, 2019.
- [35] Konstantinov, A. V. and Utkin, L. V. A new computationally simple approach for implementing neural networks with output hard constraints. In *Doklady Mathematics*, volume 108, pp. S233–S241. Springer, 2023.
- [36] Kratsios, A., Zamanlooy, B., Liu, T., and Dokmanić, I. Universal approximation under constraints is possible with transformers. *arXiv preprint arXiv:2110.03303*, 2021.
- [37] Leshno, M., Lin, V. Y., Pinkus, A., and Schocken, S. Multilayer feedforward networks with a nonpolynomial activation function can approximate any function. *Neural networks*, 6(6): 861–867, 1993.
- [38] Li, X., Deng, J., Wu, J., Zhang, S., Li, W., and Wang, Y.-G. Physical informed neural networks with soft and hard boundary constraints for solving advection-diffusion equations using fourier expansions. *Computers & Mathematics with Applications*, 159:60–75, 2024. ISSN 0898-1221. doi: <https://doi.org/10.1016/j.camwa.2024.01.021>.
- [39] Lin, T. and Zha, H. Riemannian manifold learning. *IEEE transactions on pattern analysis and machine intelligence*, 30(5):796–809, 2008.
- [40] Liu, C., Arnon, T., Lazarus, C., Strong, C., Barrett, C., and Kochenderfer, M. J. Algorithms for verifying deep neural networks. *Foundations and Trends® in Optimization*, 4(3-4):244–404, 2021. ISSN 2167-3888. doi: 10.1561/24000000035.
- [41] Lu, Z., Pu, H., Wang, F., Hu, Z., and Wang, L. The expressive power of neural networks: A view from the width. *Advances in neural information processing systems*, 30, 2017.
- [42] Manhaeve, R., Dumancic, S., Kimmig, A., Demeester, T., and De Raedt, L. Deepproblog: Neural probabilistic logic programming. *Advances in neural information processing systems*, 31, 2018.
- [43] Márquez-Neila, P., Salzmann, M., and Fua, P. Imposing hard constraints on deep networks: Promises and limitations. *arXiv preprint arXiv:1706.02025*, 2017.
- [44] McNeil, A. J., Frey, R., and Embrechts, P. *Quantitative risk management: concepts, techniques and tools-revised edition*. Princeton university press, 2015.
- [45] Min, Y., Richards, S. M., and Azizan, N. Data-driven control with inherent lyapunov stability. In *2023 62nd IEEE Conference on Decision and Control (CDC)*, pp. 6032–6037. IEEE, 2023.
- [46] Oktay, O., Ferrante, E., Kamnitsas, K., Heinrich, M., Bai, W., Caballero, J., Cook, S. A., De Marvao, A., Dawes, T., O’Regan, D. P., et al. Anatomically constrained neural networks (acnns): application to cardiac image enhancement and segmentation. *IEEE transactions on medical imaging*, 37(2):384–395, 2017.
- [47] Park, S., Yun, C., Lee, J., and Shin, J. Minimum width for universal approximation. In *International Conference on Learning Representations*, 2021.
- [48] Pathak, D., Krahenbuhl, P., and Darrell, T. Constrained convolutional neural networks for weakly supervised segmentation. In *Proceedings of the IEEE international conference on computer vision*, pp. 1796–1804, 2015.
- [49] Pinkus, A. Approximation theory of the MLP model in neural networks. *Acta numerica*, 8: 143–195, 1999.

- [50] Pryor, C., Dickens, C., Augustine, E., Albalak, A., Wang, W. Y., and Getoor, L. Neupsl: neural probabilistic soft logic. In *Proceedings of the Thirty-Second International Joint Conference on Artificial Intelligence*, pp. 4145–4153, 2023.
- [51] Qin, C., Dvijotham, K. D., O’Donoghue, B., Bunel, R., Stanforth, R., Goyal, S., Uesato, J., Swirszcz, G., and Kohli, P. Verification of non-linear specifications for neural networks. In *International Conference on Learning Representations*, 2019.
- [52] Raissi, M., Perdikaris, P., and Karniadakis, G. E. Physics-informed neural networks: A deep learning framework for solving forward and inverse problems involving nonlinear partial differential equations. *Journal of Computational physics*, 378:686–707, 2019.
- [53] Ryu, H., Lee, H.-i., Lee, J.-H., and Choi, J. Equivariant descriptor fields: Se (3)-equivariant energy-based models for end-to-end visual robotic manipulation learning. *arXiv preprint arXiv:2206.08321*, 2022.
- [54] Shao, Y. S., Chen, C., Kousik, S., and Vasudevan, R. Reachability-based trajectory safeguard (rts): A safe and fast reinforcement learning safety layer for continuous control. *IEEE Robotics and Automation Letters*, 6(2):3663–3670, 2021.
- [55] Simeonov, A., Du, Y., Tagliasacchi, A., Tenenbaum, J. B., Rodriguez, A., Agrawal, P., and Sitzmann, V. Neural descriptor fields: Se (3)-equivariant object representations for manipulation. In *2022 International Conference on Robotics and Automation (ICRA)*, pp. 6394–6400. IEEE, 2022.
- [56] Sotoudeh, M. and Thakur, A. V. Provable repair of deep neural networks. In *Proceedings of the 42nd ACM SIGPLAN International Conference on Programming Language Design and Implementation*, pp. 588–603, 2021.
- [57] Stoian, M. C., Giunchiglia, E., and Lukasiewicz, T. Exploiting t-norms for deep learning in autonomous driving. In *International Workshop on NeuralSymbolic Learning and Reasoning*, 2023.
- [58] Stoian, M. C., Dyrnishi, S., Cordy, M., Lukasiewicz, T., and Giunchiglia, E. How realistic is your synthetic data? constraining deep generative models for tabular data. In *The Twelfth International Conference on Learning Representations*, 2024.
- [59] Tang, S., Sapsis, T., and Azizan, N. Learning chaotic dynamics with embedded dissipativity. *arXiv preprint arXiv:2410.00976*, 2024.
- [60] Tao, Z. and Thakur, A. Provable editing of deep neural networks using parametric linear relaxation. In *The Thirty-eighth Annual Conference on Neural Information Processing Systems*, 2024.
- [61] Tayal, M., Goswami, B. G., Rajgopal, K., Singh, R., Rao, T., Keshavan, J., Jagtap, P., and Kolathaya, S. A collision cone approach for control barrier functions. *arXiv preprint arXiv:2403.07043*, 2024.
- [62] Tjeng, V., Xiao, K. Y., and Tedrake, R. Evaluating robustness of neural networks with mixed integer programming. In *International Conference on Learning Representations*, 2019.
- [63] Tordesillas, J., How, J. P., and Hutter, M. Rayen: Imposition of hard convex constraints on neural networks. *arXiv preprint arXiv:2307.08336*, 2023.
- [64] van Krieken, E., Thanapalasingam, T., Tomczak, J., Van Harmelen, F., and Ten Teije, A. A-nesi: A scalable approximate method for probabilistic neurosymbolic inference. *Advances in Neural Information Processing Systems*, 36:24586–24609, 2023.
- [65] Wabersich, K. P., Hewing, L., Carron, A., and Zeilinger, M. N. Probabilistic model predictive safety certification for learning-based control. *IEEE Transactions on Automatic Control*, 67(1): 176–188, 2022. doi: 10.1109/TAC.2021.3049335.
- [66] Wang, R., Zhang, Y., Guo, Z., Chen, T., Yang, X., and Yan, J. Linsatnet: the positive linear satisfiability neural networks. In *International Conference on Machine Learning*, pp. 36605–36625. PMLR, 2023.

- [67] Wang, X. and Yan, W. Q. Human identification based on gait manifold. *Applied Intelligence*, 53(5):6062–6073, 2023.
- [68] Xu, J., Zhang, Z., Friedman, T., Liang, Y., and Broeck, G. A semantic loss function for deep learning with symbolic knowledge. In *International conference on machine learning*, pp. 5502–5511. PMLR, 2018.

A Appendix

A.1 Proof of Proposition 4.2

Proof. We simplify the notation of the partition by $(\cdot)_1 := (\cdot)_{(:n_{\text{eq}})}$ and $(\cdot)_2 := (\cdot)_{(n_{\text{eq}})}$. Then,

$$A(x)\mathcal{P}(f_\theta)(x) = A_1\mathcal{P}(f_\theta)_1 + A_2\mathcal{P}(f_\theta)_2 \quad (13)$$

$$= A_1C_1^{-1}(d - C_2f_\theta^*) + A_2f_\theta^* \quad (14)$$

$$= (A_2 - A_1C_1^{-1}C_2)f_\theta^* + A_1C_1^{-1}d \quad (15)$$

$$= \tilde{A}f_\theta^* - \tilde{b} + b \quad (16)$$

$$= \tilde{A}f_\theta - \text{ReLU}(\tilde{A}f_\theta - \tilde{b}) - \tilde{b} + b \leq \tilde{b} - \tilde{b} + b = b(x). \quad (17)$$

This shows (i). For (ii),

$$C(x)\mathcal{P}(f_\theta)(x) = C_1\mathcal{P}(f_\theta)_1 + C_2\mathcal{P}(f_\theta)_2 = (d - C_2f_\theta^*) + C_2f_\theta^* = d(x). \quad (18)$$

For (iii), we first observe that

$$a_i^\top \bar{f}_\theta(x) \leq b_{(i)}(x) \iff a_{i1}^\top f_\theta + a_{i2}^\top C_2^{-1}(d - C_1f_\theta) \leq b_{(i)} \iff \tilde{a}_i^\top f_\theta \leq \tilde{b}_{(i)}. \quad (19)$$

Then, if $a_i^\top \bar{f}_\theta(x) \leq b_{(i)}(x)$,

$$a_i^\top \mathcal{P}(f_\theta)(x) = a_{i1}^\top \mathcal{P}(f_\theta)_1 + a_{i2}^\top \mathcal{P}(f_\theta)_2 \quad (20)$$

$$= (a_{i2}^\top - a_{i1}^\top C_1^{-1}C_2)f_\theta^* + a_{i1}^\top C_1^{-1}d \quad (21)$$

$$= (a_{i2}^\top - a_{i1}^\top C_1^{-1}C_2)f_\theta + a_{i1}^\top C_1^{-1}d = a_i^\top \bar{f}_\theta(x), \quad (22)$$

where the second last equality is from $\tilde{A}f_\theta^* = \tilde{A}f_\theta - \text{ReLU}(\tilde{A}f_\theta - \tilde{b})$ and $\tilde{a}_i^\top f_\theta \leq \tilde{b}_{(i)}$. Similarly, if $a_i^\top \bar{f}_\theta(x) > b_{(i)}(x)$,

$$a_i^\top \mathcal{P}(f_\theta)(x) = (a_{i2}^\top - a_{i1}^\top C_1^{-1}C_2)f_\theta^* + a_{i1}^\top C_1^{-1}d = \tilde{b}_{(i)} + a_{i1}^\top C_1^{-1}d = b_{(i)}(x) \quad (23)$$

□

A.2 Proof of Theorem 4.5

Proof. We first show that $\|f(x) - \mathcal{P}(f_\theta)(x)\|_2$ can be bounded by some constant times $\|f_{(n_{\text{eq}})}(x) - f_\theta(x)\|_2$. From (7),

$$\|f(x) - \mathcal{P}(f_\theta)(x)\|_2^2 = \|f_{(:n_{\text{eq}})}(x) - \mathcal{P}(f_\theta)_{(:n_{\text{eq}})}(x)\|_2^2 + \|f_{(n_{\text{eq}})}(x) - \mathcal{P}(f_\theta)_{(n_{\text{eq}})}(x)\|_2^2 \quad (24)$$

$$= \|C_{(:n_{\text{eq}})}^{-1}C_{(n_{\text{eq}})}(f_{(n_{\text{eq}})} - f_\theta^*)\|_2^2 + \|f_{(n_{\text{eq}})} - f_\theta^*\|_2^2 \quad (25)$$

$$\leq (1 + \|C_{(:n_{\text{eq}})}^{-1}C_{(n_{\text{eq}})}\|_2^2)\|f_{(n_{\text{eq}})} - f_\theta^*\|_2^2, \quad (26)$$

where the second equality holds by substituting $f_{(:n_{\text{eq}})}$ in (5). Meanwhile,

$$\|f_{(n_{\text{eq}})} - f_\theta^*\|_2 \leq \|f_{(n_{\text{eq}})} - f_\theta\|_2 + \|\tilde{A}^+ \text{ReLU}(\tilde{A}f_\theta - \tilde{b})\|_2 \quad (27)$$

$$\leq \|f_{(n_{\text{eq}})} - f_\theta\|_2 + \|\tilde{A}^+\|_2 \|\text{ReLU}(\tilde{A}f_{(n_{\text{eq}})} - \tilde{b} + \tilde{A}(f_\theta - f_{(n_{\text{eq}})}))\|_2 \quad (28)$$

$$\leq \|f_{(n_{\text{eq}})} - f_\theta\|_2 + \|\tilde{A}^+\|_2 \|\tilde{A}(f_\theta - f_{(n_{\text{eq}})})\|_2 \quad (29)$$

$$\leq (1 + \|\tilde{A}^+\|_2 \|\tilde{A}\|_2) \|f_{(n_{\text{eq}})} - f_\theta\|_2. \quad (30)$$

Then, putting them together, we obtain

$$\|f(x) - \mathcal{P}(f_\theta)(x)\|_2 \leq (1 + \|\tilde{A}^+\|_2 \|\tilde{A}\|_2) \sqrt{(1 + \|C_{(:n_{\text{eq}})}^{-1}C_{(n_{\text{eq}})}\|_2^2)} \|f_{(n_{\text{eq}})}(x) - f_\theta(x)\|_2. \quad (31)$$

Since $A(x), C(x)$ are continuous over the compact domain \mathcal{X} , there exists some constant $K > 0$ s.t.

$$(1 + \|\tilde{A}^+\|_2 \|\tilde{A}\|_2) \sqrt{(1 + \|C_{(:n_{\text{eq}})}^{-1}C_{(n_{\text{eq}})}\|_2^2)} \leq K \quad (32)$$

for all $x \in \mathcal{X}$. Thus,

$$\|f(x) - \mathcal{P}(f_\theta)(x)\|_2 \leq K \|f_{(n_{\text{eq}})}(x) - f_\theta(x)\|_2 \quad (33)$$

Extending the inequalities to general ℓ^p -norm for $p \geq 1$ by using the inequalities $\|v\|_q \leq \|v\|_r \leq m^{\frac{1}{r} - \frac{1}{q}} \|v\|_q$ for any $v \in \mathbb{R}^m$ and $q \geq r \geq 1$,

$$\|f(x) - \mathcal{P}(f_\theta)(x)\|_p \leq (n_{\text{out}} - n_{\text{eq}})^{\frac{1}{p} - \frac{1}{2}} K \|f_{(n_{\text{eq}})}(x) - f_\theta(x)\|_p \quad (34)$$

Then, f_θ being dense in $L^p(\mathcal{X}, \mathbb{R}^{n_{\text{out}} - n_{\text{eq}}})$ implies $\mathcal{P}(f_\theta)$ being dense in $L^p(\mathcal{X}, \mathbb{R}^{n_{\text{out}}})$. Thus, we can employ any universal approximation theorem for f_θ and convert it to that for $\mathcal{P}(f_\theta)$. We utilize Theorem 3.2 in this theorem. \square

A.3 Proof of Theorem 4.6

Proof. Similarly to the proof of Theorem 4.5 in Appendix A.2, we first prove the following inequality:

$$\|f(x) - \mathcal{P}(f_\theta)(x)\|_2 \leq \|f(x) - f_\theta(x)\|_2 \quad \forall x \in \mathcal{X}. \quad (35)$$

Given $x \in \mathcal{X}$, consider the simple case $f_\theta(x) \in \mathcal{C}(x)$ first. Then, $\mathcal{P}(f_\theta)(x) = f_\theta(x)$ from the projection in (8) which satisfies $\|f(x) - \mathcal{P}(f_\theta)(x)\|_2 \leq \|f(x) - f_\theta(x)\|_2$.

On the other hand, if $f_\theta(x) \notin \mathcal{C}(x)$, consider the triangle connecting $f_\theta(x)$, $\mathcal{P}(f_\theta)(x)$ and $f(x)$. Then, the side between $f_\theta(x)$ and $\mathcal{P}(f_\theta)(x)$ is orthogonal to the tangent hyperplane of the convex set $\mathcal{C}(x)$ at $\mathcal{P}(f_\theta)(x)$. For the two half-spaces separated by the tangent hyperplane, $f(x)$ belongs to the other half-space than the one that contains $f_\theta(x)$ since $\mathcal{C}(x)$ is convex. Thus, the vertex angle at $\mathcal{P}(f_\theta)(x)$ is larger than $\pi/2$. This implies that the side between $f_\theta(x)$ and $f(x)$ is the longest side of the triangle, so $\|f(x) - \mathcal{P}(f_\theta)(x)\|_2 \leq \|f(x) - f_\theta(x)\|_2$.

Then, We can extend this ℓ^2 -norm result to general ℓ^p -norm for $p \geq 1$ as in Appendix A.2:

$$\|f(x) - \mathcal{P}(f_\theta)(x)\|_p \leq n_{\text{out}}^{\frac{1}{p} - \frac{1}{2}} \|f(x) - f_\theta(x)\|_p. \quad (36)$$

Thus, f_θ being dense in $L^p(\mathcal{X}, \mathbb{R}^{n_{\text{out}}})$ implies $\mathcal{P}(f_\theta)$ being dense in $L^p(\mathcal{X}, \mathbb{R}^{n_{\text{out}}})$, and we can employ any universal approximation theorem for f_θ and convert it to that for $\mathcal{P}(f_\theta)$. We utilize Theorem 3.2 in this theorem. \square

A.4 Gradient Properties of HardNet-Aff

This section investigates how the enforcement layer in HardNet-Aff affects gradient computation. For simplicity, we focus on the case where $n_{\text{eq}} = 0$ (i.e., no equality constraints). For a datapoint (x, y) , consider the loss function $\ell(\mathcal{P}(f_\theta(x)), y)$. Using the chain rule, the gradient is given by:

$$\nabla_\theta \ell(\mathcal{P}(f_\theta(x)), y)^\top = \frac{\partial \ell(\mathcal{P}(f_\theta(x)), y)}{\partial \mathcal{P}(f_\theta(x))} \frac{\partial \mathcal{P}(f_\theta(x))}{\partial f_\theta(x)} \frac{\partial f_\theta(x)}{\partial \theta}. \quad (37)$$

Here, the Jacobian of the enforcement layer $\frac{\partial \mathcal{P}(f_\theta(x))}{\partial f_\theta(x)} \in \mathbb{R}^{m \times m}$ plays a key role. Let $v_i := \mathbb{1}\{a_i(x)^\top f_\theta(x) > b_{(i)}(x)\}$ indicate whether the i -th constraint is violated by $f_\theta(x)$. Then,

$$\frac{\partial \mathcal{P}(f_\theta(x))}{\partial f_\theta(x)} = I - A^+ \begin{bmatrix} v_1 a_1^\top \\ \vdots \\ v_{n_{\text{ineq}}} a_{n_{\text{ineq}}}^\top \end{bmatrix}. \quad (38)$$

Two critical properties of this Jacobian can lead to zero gradient in (37). First, if the number of constraints equals the output dimension ($n_{\text{ineq}} = m$) and all constraints are violated ($v_i = 1 \forall i$), then the Jacobian becomes zero, causing the gradient (37) to vanish. Note that this issue never happens when $n_{\text{ineq}} < m$. Second, for each $i \in \{1, 2, \dots, n_{\text{ineq}}\}$, the following holds:

$$a_i^\top \frac{\partial \mathcal{P}(f_\theta(x))}{\partial f_\theta(x)} = a_i^\top - a_i^\top A^+ \begin{bmatrix} v_1 a_1^\top \\ \vdots \\ v_{n_{\text{ineq}}} a_{n_{\text{ineq}}}^\top \end{bmatrix} = a_i^\top - e_i^\top \begin{bmatrix} v_1 a_1^\top \\ \vdots \\ v_{n_{\text{ineq}}} a_{n_{\text{ineq}}}^\top \end{bmatrix} = a_i^\top - v_i a_i^\top. \quad (39)$$

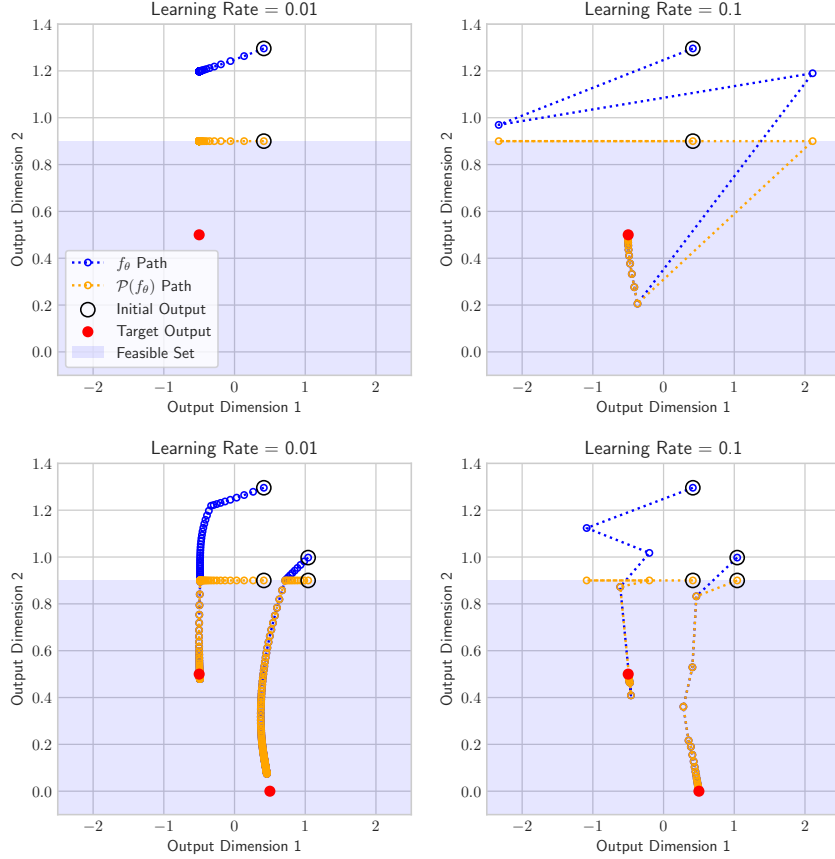


Figure 5: Visualization of 100 gradient descent steps for training a **HardNet-Aff** model on a single datapoint (first row) and two datapoints (second row) from the same initialization, using two different learning rates (0.01 and 0.1). With the smaller learning rate, training on a single datapoint results in a zero gradient due to the enforcement layer (top left). However, when training on both datapoints, the vanishing gradient for the first datapoint is mitigated by the nonzero gradient from the second datapoint (bottom left). Also, using the larger learning rate enables the model to avoid the vanishing gradient issue, even when trained on the single datapoint (top right).

This implies that if the gradient of the loss with respect to the projected output, $\left(\frac{\partial \ell(\mathcal{P}(f_\theta(x)), y)}{\partial \mathcal{P}(f_\theta(x))}\right)^\top \in \mathbb{R}^m$, lies in the span of $\{a_i | i \in \{1, \dots, n_{\text{ineq}}\}, v_i = 1\}$, then the overall gradient (37) becomes zero. This case in fact subsumes the first case, as when $n_{\text{ineq}} = m$ and $v_i = 1 \forall i$, the constraint vectors set spans the entire output space \mathbb{R}^m . However, such cases are infrequent in practical settings, particularly when the model is trained on batched data. Even when zero gradients occur for certain datapoints, they can be offset by nonzero gradients from the other datapoints within the batch. This averaging effect allows the model to update in a direction that decreases the overall loss function, mitigating the issue effectively.

We demonstrate the gradient behaviors discussed earlier using simple simulations of training **HardNet-Aff** with the conventional gradient-descent algorithm. Consider two datapoints: $d_1 = (-1, [-0.5, 0.5]^\top)$ and $d_2 = (1, [0.5, 0]^\top)$, and a neural network $f_\theta : \mathbb{R} \rightarrow \mathbb{R}^2$ with two hidden layers, each containing 10 neurons with ReLU activations. The model enforces the input-independent constraint $[0, 1] \mathcal{P}(f_\theta)(x) \leq 0.9$ using **HardNet-Aff**. Starting from the same initialization, the model is trained to minimize the squared error loss, first on d_1 alone and then on both datapoints, using two different learning rates (0.01 and 0.1), as shown in Fig. 5.

Initially, f_θ violates the constraint on both datapoints. When trained on d_1 alone with a learning rate of 0.01, the optimization path converges to a point where the gradient of the loss w.r.t. the

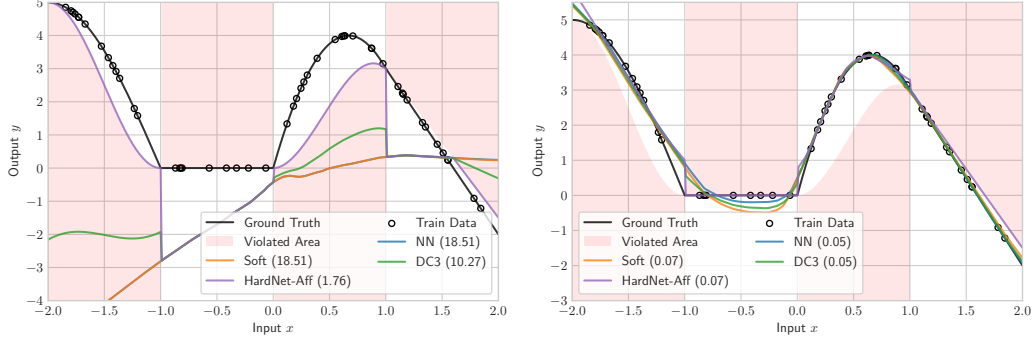


Figure 6: Learned functions at the initial (left) and final (right) epochs for the function fitting experiment. The models are trained on the samples indicated with circles, with their MSE distances from the true function shown in parentheses. **HardNet-Aff** adheres to the constraints from the start of the training. On the other hand, the baselines violate the constraints throughout the training.

projected output is orthogonal to the gradient boundary, causing the overall gradient (37) to vanish. However, when the model is trained on both datapoints, the vanishing gradient for d_1 is mitigated by the nonzero gradient for d_2 , enabling the model to achieve target values strictly within the feasible set. Furthermore, using a larger learning rate (0.1) allows the model to avoid the vanishing gradient issue and reach the target value even when trained solely on d_1 .

A.5 Learning with Warm Start

In addition to the **HardNet** architecture shown in Figure 1 that consists of a neural network f_θ and a differentiable enforcement layer with a projection \mathcal{P} appended at the end, we propose a training scheme that can potentially result in better-optimized models. For the first k epochs of training, we disable the enforcement layer and train the plain neural network f_θ . Then, from the $(k+1)$ -th epoch, we train on the projected model $\mathcal{P}(f_\theta)$. During the k epochs of warm start, the neural network f_θ can be trained in a soft-constrained manner by regularizing the violations of constraints. In this paper, we train the **HardNet-Aff** models without the warm-start scheme for simplicity.

A.6 Details for the Learning with Piecewise Constraints Experiment

The target function and constraints are as below:

$$f(x) = \begin{cases} -5 \sin \frac{\pi}{2}(x+1) & \text{if } x \leq -1 \\ 0 & \text{if } x \in (-1, 0] \\ 4 - 9(x - \frac{2}{3})^2 & \text{if } x \in (0, 1] \\ 5(1-x) + 3 & \text{if } x > 1 \end{cases}, \text{ Constraints: } \begin{cases} y \geq 5 \sin^2 \frac{\pi}{2}(x+1) & \text{if } x \leq -1 \\ y \leq 0 & \text{if } x \in (-1, 0] \\ y \geq (4 - 9(x - \frac{2}{3})^2)x & \text{if } x \in (0, 1] \\ y \leq 4.5(1-x) + 3 & \text{if } x > 1 \end{cases}. \quad (40)$$

These four constraints can be aggregated into the following single affine constraint:

$$a(x)y \leq b(x) : \begin{cases} a(x) = -1, b(x) = -5 \sin^2 \frac{\pi}{2}(x+1) & \text{if } x \leq -1 \\ a(x) = 1, b(x) = 0 & \text{if } x \in (-1, 0] \\ a(x) = -1, b(x) = (9(x - \frac{2}{3})^2 - 4)x & \text{if } x \in (0, 1] \\ a(x) = 1, b(x) = 4.5(1-x) + 3 & \text{if } x > 1 \end{cases}. \quad (41)$$

The results in Section 5.1 show **HardNet-Aff** can help generalization on unseen regimes by enforcing constraints. In this section, we provide additional results that train the models on data spanning the entire domain of interest $[-2, 2]$. As shown in Figure 6 and Table 5, the models exhibit similar generalization performances while **HardNet-Aff** satisfy the constraints throughout the training.

Table 5: Results for the function fitting experiment. **HardNet-Aff** attains a comparable MSE distance from the true function as other methods without any constraint violation. The max, mean, and the number of constraint violations are computed out of 401 test samples. Violations are highlighted in red. Standard deviations over 5 runs are shown in parentheses.

| | MSE | $\not\leq$ max | $\not\leq$ mean | $\not\leq$ # | T_{test} (ms) | T_{train} (s) |
|-------------|-------------|--------------------|--------------------|---------------------|------------------------|------------------------|
| NN | 0.04 (0.01) | 0.73 (0.07) | 0.02 (0.01) | 42.40 (5.31) | 1.54 (0.02) | 2.45 (0.80) |
| Soft | 0.05 (0.01) | 0.69 (0.04) | 0.02 (0.00) | 28.60 (2.42) | 1.82 (0.37) | 2.54 (0.87) |
| DC3 | 0.04 (0.01) | 0.48 (0.03) | 0.01 (0.00) | 30.60 (1.85) | 50.99 (0.11) | 14.43 (0.99) |
| HardNet-Aff | 0.06 (0.01) | 0.00 (0.00) | 0.00 (0.00) | 0.00 (0.00) | 7.04 (0.23) | 4.85 (0.78) |

A.7 Details for the Safe Control Experiment

In this experiment, we consider controlling a unicycle system with system state $x = [x_p, y_p, \theta, v, w]^\top$ which represents the pose, linear velocity, and angular velocity. The dynamics of the unicycle system is given by

$$\begin{bmatrix} \dot{x}_p \\ \dot{y}_p \\ \dot{\theta} \\ \dot{v} \\ \dot{w} \end{bmatrix} = \begin{bmatrix} v \cos \theta \\ v \sin \theta \\ w \\ 0 \\ 0 \end{bmatrix} + \begin{bmatrix} 0 & 0 \\ 0 & 0 \\ 0 & 0 \\ 1 & 0 \\ 0 & 1 \end{bmatrix} \begin{bmatrix} a_{\text{lin}} \\ a_{\text{ang}} \end{bmatrix}, \quad (42)$$

with the linear and angular accelerations $a_{\text{lin}}, a_{\text{ang}}$ as the control inputs.

To avoid an elliptical obstacle centered at (c_x, c_y) with its radii r_x, r_y , one could consider the following CBF candidate:

$$h_{\text{ellipse}}(x) = \left(\frac{c_x - (x_p + l \cos \theta)}{r_x} \right)^2 + \left(\frac{c_y - (y_p + l \sin \theta)}{r_y} \right)^2 - 1, \quad (43)$$

where l is the distance of the body center from the differential drive axis of the unicycle system. However, it is not a valid CBF since the safety condition (10) does not depend on the control input (i.e., $\nabla h_{\text{ellipse}}(x)^\top g(x) = 0 \ \forall x$). Instead, we can exploit a higher-order CBF (HOCBF) given by

$$h(x) = \dot{h}_{\text{ellipse}}(x) + \kappa h_{\text{ellipse}}(x), \quad (44)$$

for some $\kappa > 0$. Then, ensuring $\dot{h} \geq 0$ implies $h \geq 0$ given $h(x(0)) \geq 0$, and the safety condition (10) for this h depends on both control inputs $a_{\text{lin}}, a_{\text{ang}}$. Refer to Tayal et al. [61] for a detailed explanation.

The goal of this problem is to optimize the neural network policy $\pi_\theta(x) = \pi_{\text{nom}}(x) + f_\theta(x)$ to minimize the expected cost over the trajectories from random initial points within the range from $[-4, 0, -\pi/4, 0, 0]$ to $[-3.5, 0.5, -\pi/8, 0, 0]$. For an initial state sample x_s , we consider the cost of the rolled-out trajectory through discretization with time step $\Delta t = 0.02$ and $n_{\text{step}} = 50$ as

$$\Delta t \sum_{i=0}^{n_{\text{step}}-1} x_i^\top Q x_i + \pi_\theta(x_i)^\top R \pi_\theta(x_i), \quad (45)$$

where x_i is the state after i steps, and $Q = \text{diag}(100, 100, 0, 0.1, 0.1)$ and $R = \text{diag}(0.1, 0.1)$ are diagonal matrices. The neural network policies are optimized to reduce (45) summed over 1000 randomly sampled initial points.

A.8 Additional Scenario: Airborne Collision Avoidance System (ACAS)

In this scenario, we consider learning an airborne collision avoidance system for unmanned aircraft (ACAS Xu) used by Katz et al. [32]. The goal of the system is to provide horizontal maneuver advisories—clear of conflict, weak left, strong left, weak right, strong right—to aircrafts in order to stay safe and avoid collisions. The system takes the state of the ownship and the relative state of the intruder airplane as inputs, and outputs a score for each of the 5 possible advisories listed above. Traditionally, this was accomplished using lookup tables but using neural networks has recently become customary.

In their original work, Katz et al. [32] developed a method called *Reluplex* for formally verifying that the deep neural networks used for generating the scores of the advisories always satisfy certain *hard constraints*. This requires training a model and then verifying that it satisfies the constraints by solving a satisfiability problem. Instead, we can learn neural networks that output constrained airplane advisories *by construction*, rather than engaging in an iterative cycle of training a neural network and separately verifying it until convergence. While some of the properties in the original problem [32] are non-convex in nature, we introduce five of the properties that can be encoded in a convex form below.

A.8.1 Problem Details

- **Input** - The input is a 7-dimensional vector.
 1. ρ (ft) - Range to intruder
 2. θ (radians) - Bearing angle to intruder
 3. ψ (radians) - Relative heading angle of intruder
 4. v_{own} (ft/s) - Ownship speed
 5. v_{int} (ft/s) - Intruder speed
 6. τ (s) - Time to loss of vertical separation
 7. s_{adv} - Previous advisory
- **Output** - The output is a 5-dimensional vector y of floats each of whom represent the *score* for a particular advisory (in order). We also list the ownship turn rate range corresponding to each advisory.
 1. $y[0]$: Clear-Of-Conflict (COC) : $[-1.5 \text{ deg/s}, 1.5 \text{ deg/s}]$
 2. $y[1]$: Weak Left (WL) : $[1.0 \text{ deg/s}, 2.0 \text{ deg/s}]$
 3. $y[2]$: Weak Right (WR) : $[-2.0 \text{ deg/s}, -1.0 \text{ deg/s}]$
 4. $y[3]$: Strong Left (SL) : $[2.0 \text{ deg/s}, 4.0 \text{ deg/s}]$
 5. $y[4]$: Strong Right (SR) : $[-4.0 \text{ deg/s}, -2.0 \text{ deg/s}]$
- **Constraints** -
 1. Property #1 :
 - **Description** : If the intruder is distant and is significantly slower than the ownship, the score of a COC advisory will always be below a certain fixed threshold.
 - Conditions on input for constraint to be active :
 - * $\rho \geq 55947.691$
 - * $v_{own} \geq 1145$
 - * $v_{int} \leq 60$
 - Constraints on output : $y[0] \leq 1500$
 2. Property #5 :
 - **Description** : If the intruder is near and approaching from the left, the network advises “strong right”.
 - Conditions on input for constraint to be active :
 - * $250 \leq \rho \leq 400$
 - * $0.2 \leq \theta \leq 0.4$
 - * $100 \leq v_{own} \leq 400$
 - * $0 \leq v_{int} \leq 400$
 - Constraints on output : $y[4]$ should be the minimal score which translates to $y[4] \leq \min\{y[0], y[1], y[2], y[3]\}$
 3. Property #6 :
 - **Description** : If the intruder is sufficiently far away, the network advises COC.
 - Conditions on input for constraint to be active :
 - * $12000 \leq \rho \leq 62000$
 - * $100 \leq v_{own} \leq 1200$
 - * $0 \leq v_{int} \leq 1200$

- Constraints on output : $y[0]$ should be the minimal score which translates to $y[0] \leq \min\{y[1], y[2], y[3], y[4]\}$
4. Property #9 :
- **Description** : Even if the previous advisory was “weak right”, the presence of a nearby intruder will cause the network to output a “strong left” advisory instead.
 - Conditions on input for constraint to be active :
 - * $2000 \leq \rho \leq 7000$
 - * $-0.4 \leq \theta \leq -0.14$
 - * $100 \leq v_{own} \leq 150$
 - * $0 \leq v_{int} \leq 150$
 - Constraints on output : $y[3]$ should be the minimal score which translates to $y[3] \leq \min\{y[0], y[1], y[2], y[4]\}$
5. Property #10 :
- **Description** : For a far away intruder, the network advises COC.
 - Conditions on input for constraint to be active :
 - * $36000 \leq \rho \leq 60760$
 - * $0.7 \leq \theta \leq 3.141592$
 - * $900 \leq v_{own} \leq 1200$
 - * $600 \leq v_{int} \leq 1200$
 - Constraints on output : $y[0]$ should be the minimal score which translates to $y[0] \leq \min\{y[1], y[2], y[3], y[4]\}$

A.9 Related Work in Neuro-Symbolic AI

HardNet also aligns with the objectives of Neuro-symbolic AI, a field that has gained significant attention in recent years for its ability to integrate complex background knowledge into deep learning models. Unlike HardNet, which focuses on algebraic constraints, the neuro-symbolic AI literature primarily addresses logical constraints. A common approach in this field is to *softly* impose constraints during training by introducing penalty terms into the loss function to discourage constraint violations [68, 24, 7, 57]. While these methods are straightforward to implement, they do not guarantee constraint satisfaction. In contrast, works such as Giunchiglia & Lukasiewicz [26], Ahmed et al. [2], Giunchiglia et al. [27] ensure constraints are satisfied by embedding them into the predictive layer, thus guaranteeing compliance by construction. Another line of research maps neural network outputs into logical predicates, ensuring constraint satisfaction through reasoning on these predicates [42, 50, 64].